Materials Advances

ROYAL SOCIETY OF CHEMISTRY

PAPER

View Article Online
View Journal | View Issue

Cite this: *Mater. Adv.*, 2024, 5, 2860

Preparation of a cyclotriphosphazene microsphere bearing a phosphaphenanthrene structure towards fire-safety and mechanical enhancement for epoxy and its aramid fiber composite†

Yunxian Yang, *[abc] Qi Zhang,[c] Yiwen Hao,[ac] Xuke Lan,[c] Laia Haurie,[d] Dezhi Zheng[b] and Guangyan Huang*[ac]

The mismatch of flame retardancy and mechanical properties is still a challenge for developing high-performance epoxy resin (EP) and its aramid fiber (AF) composite. In this study, a multifunctional cyclotriphosphazene microsphere EHP modified by a phosphaphenanthrene structure was prepared to solve the issue by taking advantage of multiple flame-retardant actions and interfacial interaction. After introducing EHP into epoxy resin, the thermoset exhibited good thermal stability, excellent flame retardancy and enhanced mechanical properties. Especially for sample EP/3%EHP with only 0.39 wt% P-loading, the limiting oxygen index (LOI) value increased from 25.5% to 33.5% accompanied by the V-0 rating in the UL-94 test; besides, the heat release and smoke release behaviors were also inhibited. Additionally, the tensile and impact strengths of the same epoxy sample increased by 11 MPa and 64% relative to pure epoxy resin. Moreover, compared with sample AF/EP, the incorporation of EHP improved both the burning behavior and mechanical properties of the composite, reflecting as reduced burning intensity, increased tensile strength and interlaminar shear strength. The flame-retardant actions, involving flame inhibition and charring and barrier effects, were evaluated quantitatively. Meanwhile, the strengthening and toughening effect benefitted from good compatibility and increased interface bonding.

Received 1st December 2023,
Accepted 2nd February 2024

DOI: 10.1039/d3ma01074k

rsc.li/materials-advances

1. Introduction

Thanks to excellent mechanical properties and strong adhesion, epoxy resin (EP) exhibits exclusive application in fabricating fiber reinforced plastic materials.[1,2] Amongst them, aramid fiber reinforced epoxy resin composites (AF/EP) are developed to meet different industrial requirements.[3] However, the intrinsic flammability of EP has become a key factor that restricts its further application, and also brings about fire risk for AF/EP composites due to the wick effect, in which the heat and fuel are produced and transferred along the fiber direction to continuously feed the fire.[4–7] In most cases, the flame retardancy of EP was improved, which was always accompanied by the deterioration of mechanical properties due to the negative interaction between EP and flame retardants.[8–10] Therefore, achieving good flame retardancy and maintaining excellent mechanical properties are the hotspots for EP and AF/EP.

In order to satisfy the requirements of flame resistance and environmental benign, various phosphorus-containing flame retardants (P-FRs) have been designed to prepare efficient flame retardants for epoxy resin with good comprehensive performance.[11] The dominant mechanism of P-FRs comprises actions in condensed and gas phases, which depends on different chemical structures.[12] Hexachlorocyclotriphosphazene (HCCP) is a heterocyclic ring (P=N) structure consisting of phosphorus and nitrogen atoms, which is conducive to promoting the flame-retardant effect in the condensed phase.[13,14] Furthermore, the six chemically active chlorine atoms of HCCP can be easily substituted by other functional groups *via* nucleophilic reactions,[15,16] and some derivatives have been prepared to investigate the effect on epoxy resin. For example, HCCP was used to modify lignin to enhance the barrier effect of epoxy composites,[17] and 58.9% and 63.1% reduction were observed in

[a] *State Key Laboratory of Explosion Science and Safety Protection, Beijing Institute of Technology, Beijing 100081, P. R. China. E-mail: yunxian.yang@bit.edu.cn, huanggy@bit.edu.cn*
[b] *Advanced Research Institute of Multidisciplinary Sciences, Beijing Institute of Technology, Beijing 100081, P. R. China*
[c] *Chongqing Innovation Center, Beijing Institute of Technology, Chongqing, 401120, P. R. China*
[d] *Department of Tecnologia de l'Arquitectura, Universitat Politècnica de Catalunya, Av. Dr Marañon 44-50, 08028, Barcelona, Spain*

† Electronic supplementary information (ESI) available. See DOI: https://doi.org/10.1039/d3ma01074k

heat and smoke release processes, respectively. After incorporating the cyclotriphosphazene ring into the 3D crosslinked network,[18] the epoxy resin demonstrated 31% LOI value and UL-94 V-0 rating, which was much better than that of bisphenol A diglycidyl ether (DGEBA)-based epoxy systems. The increased char yield and intumescent behavior accounted for the outstanding flame retardation of the cyclotriphosphazene structure. Besides, HCCP was also combined with halloysite nanotubes[19] or carbon nanotubes[20] to fabricate flame-retardant epoxy resins *via* amplifying actions in the condensed phase.

Another phosphorus-containing compound with a phosphaphenanthrene structure, named 9,10-dihydro-9-oxa-10-phosphaphenanthrene-10-oxide (DOPO), exhibits remarkable gas-phase flame-retardant action and has been used as a starting material to synthesize efficient flame retardant for epoxy resin. With regard to the effect on other performances of epoxy resin, the rigid group in DOPO is beneficial to achieve good thermal stability and mechanical properties.[21] Moreover, aramid fiber presents an obvious inert surface, and the interface interaction between the matrix and fiber plays a key role in the final performance of the AF/EP composite.[22,23] Therefore, as for EP and AF/EP, it is possible to achieve efficient flame retardancy *via* strong synergism of these two multiple groups. Simultaneously, HCCP with a microsphere structure has high specific surface area and can be modified by organic side groups, which would improve the dispersion and compatibility of the filler in the matrix. Consequently, the enhanced mechanical properties can also be obtained through optimizing interfacial interactions.[24,25]

Aiming to solve the mismatch of flame retardancy and mechanical properties, this study designed a multifunctional flame retardant (EHP) containing cyclotriphosphazene and phosphaphenanthrene structures, which would exhibit some advantages for EP and AF/EP composites as follows: (1) the synergistic effect can be achieved by taking advantages of multiple actions in gas and condensed phases; (2) the charring behavior would be facilitated by catalyzing the formation of more cross-linking structures during temperature elevation; (3) high thermal stability can be maintained due to the rigid structures; (4) the deterioration of mechanical properties would be solved *via* the micro size effect. Overall, EHP is a kind of cyclotriphosphazene microsphere with inorganic and organic components, which can result in the enhancement in both flame retardancy and mechanical properties. The positive effects of EHP on EP and AF/EP composites were noticed in terms of thermal stability, flame retardancy and mechanical properties. The flame-retardant mechanism was evaluated quantitatively, and the mechanical enhancement mechanism was investigated *via* analyzing the interface performance.

2. Experimental

2.1. Materials

Aramid fabric (PF-J09, plain-weave) with areal density of 200 g m^{-2} and thickness of 0.33 mm was kindly supplied by Hunan Air Defense Technology Co., Ltd, China. The thread count of warp and weft yarns is 106 yarns per 10 cm, and the tensile strengths of warp and weft yarns are 9090 N per 5 cm and 10 010 N per 5 cm, respectively. Epoxy resin (DGEBA: epoxy value of 0.51 mol/100 g) was provided by Guangzhou Huixin Chemical Co., Ltd. Curing agent (DDM: 4,4-diamino-diphenylmethane), hexachlorocyclophosphazene (HCCP), triethylamine (TEA), *N*,*N*-dimethylformamide (DMF), and tetrahydrofuran (THF) were purchased from Shanghai Macklin Biochemical Co., Ltd. All the solvents and chemicals were used without further treatment. Another reactant named EAD was prepared according to the previous method.[26]

2.2. Synthesis of flame retardant EHP

The flame retardant EHP was synthesized through the reaction between the P–Cl bond and $-NH_2$ group in light of the typical method for organocyclophosphazene compounds.[27] EAD (1.67 g, 5 mmol) and HCCP (0.29 g, 0.83 mmol) were dissolved in DMF of 50 mL and THF of 22.5 mL, respectively. Afterwards, these two solutions were mixed at 0 °C during stirring, and TEA (0.56 g, 5.5 mmol) was added into the homogeneous solution. When the reaction was performed for 12 h at 80 °C under a nitrogen atmosphere, the by-product was separated by suction filtration while the crude product was collected by dropping the filtrate into excess deionized water. After washing the product with deionized water and ethanol, the yellow compound EHP with a yield of 61% was obtained through lyophilization for 24 h.

2.3. Preparation of EP and AF/EP samples

The EP thermosets were prepared as follows: firstly, flame retardant EHP was mixed with epoxy resin by a three-roll mill (BUNKIN BS65, China); then, curing agent DDM was added into the well-dispersed system; finally, the homogeneous system was cured at 100 °C for 2 h and 150 °C for 2 h in the PTFE mold. The EHP content in EP was fixed at 1 wt%, 3 wt%, and 5 wt%, and the corresponding EP samples were named EP/1%EHP, EP/3%EHP, and EP/5%EHP, respectively. Besides, the phosphorus content was calculated according to the mass fraction of phosphorus element in the total amount of epoxy resin, and the corresponding values were 0.13 wt%, 0.39 wt%, and 0.65 wt% for samples EP/1%EHP, EP/3%EHP, and EP/5%EHP, respectively.

The AF/EP laminates were fabricated *via* hand lay-up and hot-press processes. After AF was ultrasonically treated in acetone solution for 10 min and dried at 60 °C, the well mixed epoxy resin with 9 wt% ethanol as the diluent was applied to impregnate the AF. Then, the infiltrated AF/EP prepreg was put into a hot presser as well as degassed under a pressure of 1 MPa 3 times. The cured laminate was obtained under the conditions of 3 MPa at 100 °C for 2 h and 150 °C for 2 h. Finally, the specimens with different dimensions were cut using a high velocity water jet machine (JJ-II42-2020, China). The content of EHP was set as 3 wt% and 5 wt% in the total amount of epoxy resin, which was named sample AF/EP/3%EHP and AF/EP/5%EHP, respectively. Besides, the control samples EP and AF/EP without EHP were also prepared under the same conditions, and

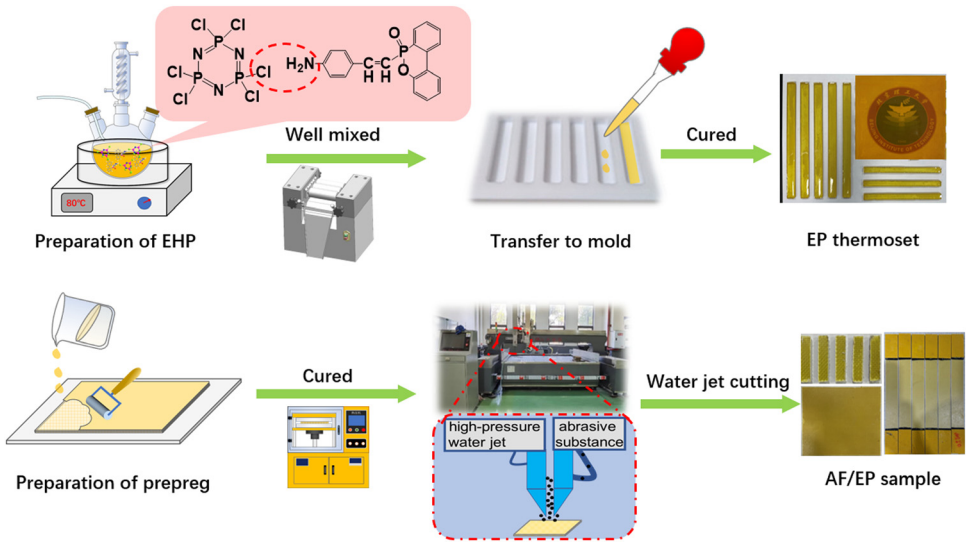

Fig. 1 Scheme of the preparation of EP and AF/EP composites.

the matrix content in the laminates was kept at 40 wt%. The fabrication process of EP and AF/EP composites is illustrated in Fig. 1.

2.4 Characterization

Chemical structure. ^{1}H NMR and ^{31}P NMR spectra of compounds were obtained on a nuclear magnetic resonance (NMR) system (Bruker Avance AV II-600 NMR) with DMSO-d6 as the solvent. Fourier transform infrared spectra (FTIR) of samples were collected in the range of 400–4000 cm^{-1} wavenumbers from a spectrometer (Thermo Nicolet iS20) in KBr mode. The morphology of EHP was also analyzed by scanning electron microscopy along with energy dispersive spectroscopy (SEM/EDS: Thermo ProX).

Curing behavior. The effect of EHP on curing behavior of epoxy resin was investigated using a rheometer (DHR10, TA). The sample for the rheological test was put between two parallel plates, and the temperature sweep measurement was performed to observe the relationship between the temperature and complex viscosity of the resins. The procedure was set in the range of 40–180 °C with a heating rate of 2 °C min^{-1}.

Thermal stability. Thermogravimetric analysis (TGA) and differential scanning calorimetry (DSC) were used to study the thermal stability of EP composites. Each sample with 10 ± 0.5 mg was heated from 30 to 700 °C at the rate of 10 °C min^{-1} under a nitrogen flow of 60.0 mL min^{-1} on a system (TGA550, TA). As for the DSC (DSC250, TA) test, epoxy resins were heated from room temperature to 250 °C under a nitrogen atmosphere with a heating rate of 10 °C min^{-1}.

Burning performance. The limiting oxygen index (LOI) (HC-2C, China) test, UL-94 vertical burning (CZF-4, China) test, and cone calorimeter test (CCT: FTT, UK) were carried out to investigate the burning behavior of EP and AF/EP composites. The dimensions of the samples were set at 127.0 mm × 6.5 mm × 3.0 mm, 127.0 mm × 13.0 mm × 3.0 mm, and 100.0 mm × 100.0 mm × 3.0 mm according to standard ASTM D 2863, ASTM D 3801, and ISO 5660, respectively. Besides, the heat flux of CCT was set at 50 kW m^{-2}. SEM, pyrolysis combustion flow calorimetry (PCFC), and TGA coupled with FTIR (TG-IR) technology were carried out to investigate the flame-retardant mechanism. SEM was conducted under a vacuum environment at a voltage of 15 kV on the same equipment. PCFC was performed in the range of 100–900 °C on an apparatus (FTT, UK) according to ASTM D 7309. The parameters of the TG-IR test were set as the same as in the procedures of single TGA and FTIR.

Mechanical properties. Tensile and interlaminar shear strength (ILSS) tests (MTS E45, USA), as well as un-notched Charpy impact (ZBC8400-B, China), were conducted to assess the mechanical properties of the composites. Standards ASTM D 628 and ASTM 3039 were followed to trial the tensile properties of EP (150.0 mm × 10.0 mm × 4.0 mm) and AF/EP (250.0 mm × 25.0 mm × 3.0 mm) samples, respectively, at a crosshead speed of 2 mm min^{-1}. Impact strength of EP thermosets (80.0 mm × 10.0 mm × 4.0 mm) was obtained according to standard ISO 179. In accordance with the ASTM D 2344 standard, ILSS of AF/EP laminates (25.0 mm × 6.0 mm × 3.0 mm) was measured in a short-beam shear mode with a span length of 12 mm and a loading speed of 1 mm min^{-1}. At least 5 specimens were loaded for each test. Moreover, the fracture surface of the EP and AF/EP composite was observed by SEM to analyze the interfacial performance.

3. Results and discussion

3.1. Characterization of EHP

First of all, the chemical structure of EHP was confirmed by the NMR method, as shown in Fig. 2(a and b). In the ^{1}H NMR spectrum of EHP, the chemical shift at 7.2–8.3 ppm was ascribed to protons in phosphaphenanthrene groups, and the signals caused by the benzene ring and vinyl group were observed at around 6.5/7.6 ppm and 6.1/6.9 ppm, respectively.

Besides, the peak at 6.0 ppm from the amino group disappeared and a new shift was detected at 6.7 ppm, which indicated that the $-NH_2$ group was converted into the –NH– group.[28,29] Different from the ^{31}P NMR spectrum of HCCP with only chemical shift at −0.4 ppm, there were two obvious signals at 25.0 ppm and 6.3 ppm in the ^{31}P NMR spectrum of EHP, which were assigned to the phosphaphenanthrene and cyclotriphosphazene structure, respectively.[30,31] Another chemical shift at around 27 ppm was caused by the different spatial configuration of DOPO. The results from ^{31}P NMR confirmed that the Cl atom was substituted by the DOPO conjugated structure.

FTIR spectra are also illustrated in Fig. 2(c) to further characterize the chemical structure of EHP. In the spectrum of EHP, absorptions at 1211 cm^{-1}, 1597 and 1477 cm^{-1} were attributed to the P=N and P–C_{Ar} stretching vibration in cyclotriphosphazene and phosphaphenanthrene rings, respectively.[32] Meanwhile, peaks at around 604 cm^{-1} and 3500 cm^{-1} from P–Cl bonds and $-NH_2$ groups almost disappeared while a new signal at 930 cm^{-1} assigned to the P–NH bond was observed,[33,34] which confirmed the reaction between P–Cl and $-NH_2$.

Moreover, the morphology of EHP was studied by SEM/EDS as shown in Fig. 2(d), which demonstrated that the EHP exhibited a microsphere shape with a size of around 2 μm. The analysis of elements' constituents from the microsphere surface also supported that EHP was prepared successfully. The data from TGA for EHP are listed in Fig. 3(c and d) and Table 1. EHP demonstrated one predominant degradation stage, and the maximum decomposition took place at 434 °C (T_{max}). Besides, the initial degradation temperature ($T_{5\,wt\%}$) and residue at 700 °C were 303 °C and 24.8%, respectively. This good thermal stability and charring behavior are attributed to the rigid structure and aromatic groups, which are also beneficial to the properties of epoxy resin.

3.2. Curing behavior of epoxy resin

The curing behavior of epoxy resin before and after modification was investigated through analyzing the relationship of viscosity and temperature, as shown in Fig. 3(a). All the epoxy

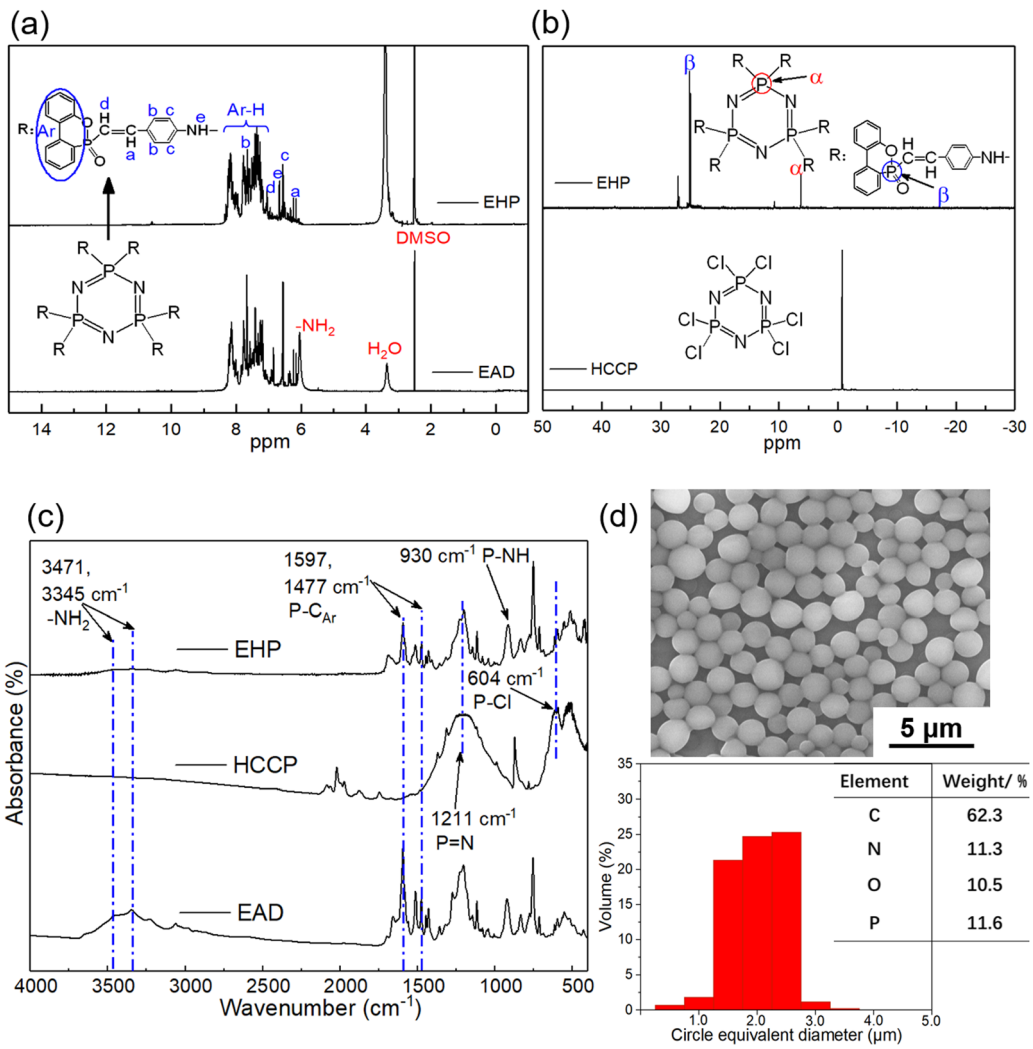

Fig. 2 Chemical structure characterization of EHP: (a) ^{1}H NMR spectra, (b) ^{31}P NMR spectra, (c) FTIR spectra, and (d) data from SEM/EDS.

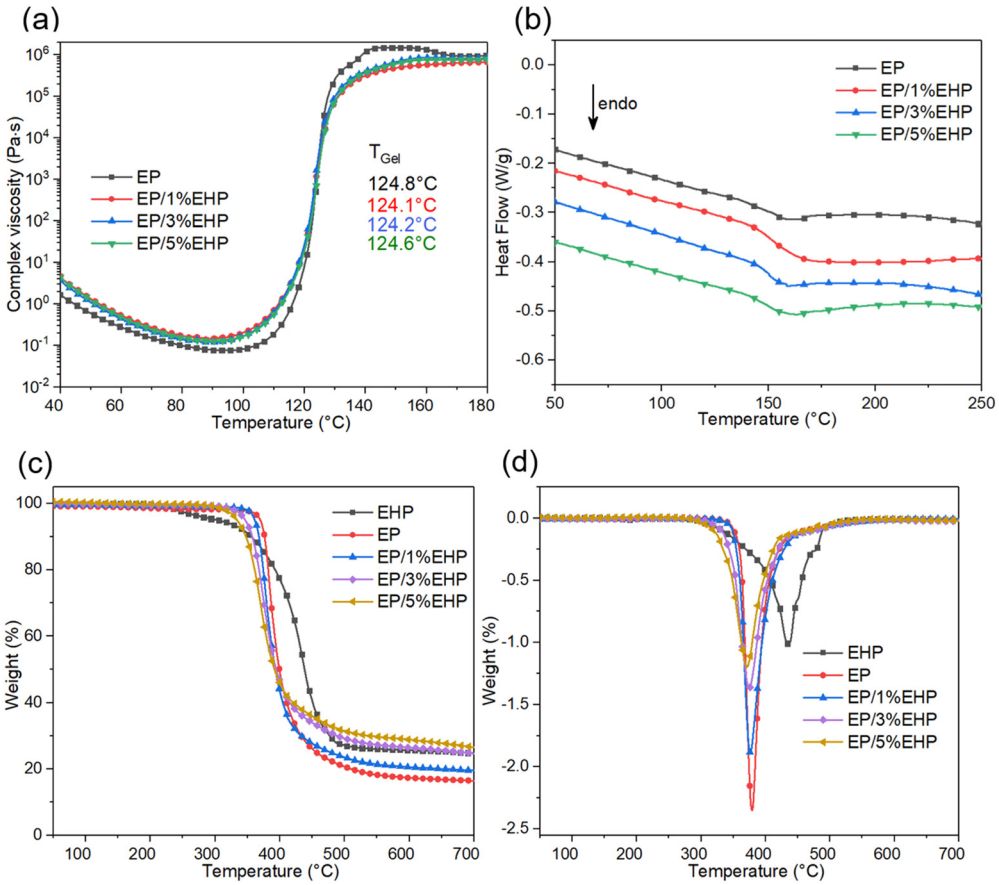

Fig. 3 Results of curing behavior and thermal stability for EP thermosets: (a) viscosity *vs.* temperature curves, (b) isothermal curves from DSC, (c) TGA curves, and (d) DTG curves.

Table 1 Results from TGA, DSC, LOI and UL-94

Sample	$T_{5\,wt\%}$ (°C)	T_{max} (°C)	Residue at 700/(%)	T_g (°C)	LOI (%)	UL-94 $\overline{t1+t2}$/(s)	UL-94 Rating
EHP	303	434	24.8	—	—	—	—
EP	365	377	16.6	157.5	25.5	Burn out	No rating
EP/1%EHP	359	376	19.6	154.9	29.0	19 + 5	V-1
EP/3%EHP	346	374	25.1	159.7	33.5	2 + 5	V-0
EP/5%EHP	334	371	26.7	167.5	34.5	1 + 2	V-0

resin systems had similar rheology behavior during the temperature elevation, presenting first a descending and then an ascending trend. 100 °C was the inflection point, before which the decreased viscosity was due to the decreased molecular interactions of epoxy resin, and after which the sharp increase was caused by the crosslinking reaction among molecules. Compared with pure epoxy resin, a little difference was observed in the viscosity of modified systems at the same temperature, and this was attributed to the catalyzing effect from hydrogen bonding of –NH structure in EHP.[35] However, the gelation temperature (T_{Gel}) was hardly altered by adding EHP. T_{Gel} can be obtained by the cross-over point of storage modulus (G') and loss modulus (G''), which are listed in Fig. S1 (ESI†). Therefore, the addition of EHP had little effect on the curing behavior of epoxy resin, and can be considered as an additive flame retardant for the resin.

3.3. Thermal stability of the EP sample

The thermal decomposition of EP samples is presented in Fig. 3(c and d). There was only a one-step degradation stage for all the thermosets during the heating process. The $T_{5\,wt\%}$ and T_{max} were defined as the temperature at 5 wt% and the maximum weight loss, respectively. Together with the residue char at 700 °C and the glass transition temperature (T_g) from DSC, listed in Fig. 3(b) and Table 1, these parameters were used to assess the thermal stability. In comparison with pure EP, the modified samples showed lower values of $T_{5\,wt\%}$ and T_{max}, which decreased with the content of EHP. The early degradation is

because EHP decomposed firstly and the products facilitated the carbonization process of matrix resin, which can slow down the subsequent degradation process. This phenomenon was confirmed by the reduced maximum decomposition rate, as well as the closing gap between the T_{max} values, which change from 377 °C of sample EP to 371 °C of sample EP/5%EHP. Furthermore, the residue of sample with 5 wt% EHP at 700 °C increased by 60.8% compared to that of the pure resin, and this demonstrated that EHP endowed epoxy resin with a good charring effect. As for T_g, related to the molecular structure of polymers,[36] the value increased after adding EHP. On the one hand, the presence of the bulk structure can restrict the movement of molecular chains, and the imino group in EHP would take part in the crosslinking reaction to create a heat stable network structure. On the other hand, the steric hindrance and limited crosslinking points from the EHP molecule can also lead to a negative effect during the crosslinking process to decrease the T_g. Therefore, the improvement of T_g in the EP/EHP system was brought on by the fact that the positive effect played a more important role than the negative effect at this loading range of EHP. Additionally, the only one endothermic peak insinuated the good compatibility in this mixed resin system.

3.4. Flame retardancy of EP and AF/EP samples

As shown in Table 1, the LOI value of EP samples increased with the content of EHP, and the afterflame time in the UL-94 test also decreased obviously for modified samples. Taking sample EP/1%EHP as an example, the flame lasted for 24 s after removing the igniter, and only 0.13% P-loading made epoxy resin pass V-1 rating. Fig. 4(a) illustrates the combustion process of EP samples. In addition to the weakening flame intensity, introducing EHP also resulted in obvious "blowing-out" phenomena. This is because EHP begins to decompose while heating, which generates not only P-containing products to quench HO• free radicals from epoxy resin but also a certain amount of non-combustible gases to blow out unstable flames. Finally, V-0 rating was achieved for both samples EP/3%EHP and EP/5%EHP with P-loading of 0.39% and 0.65%, respectively.

As a bench-scale test, the cone calorimeter test (CCT) was performed to investigate the combustion behavior of EP and AF/EP samples in these simulated fire scenarios. Some important parameters related to heat release and smoke release behavior were studied, including the heat release rate (HRR), peak heat release rate (PHRR), maximum average rate of heat emission (MARHE), total heat release (THR), total smoke production (TSP), and total smoke release (TSR). Moreover, time to ignition (TTI), average effective heat combustion (av-EHC) and residue were analyzed as well. As shown in Table 2 and Fig. 4(b and c), the presence of EHP effectively suppressed the heat release and smoke release behavior of epoxy resin during combustion. By increasing the addition of EHP, THR, PHRR, TSP and TSR decreased gradually. In comparison to sample EP, the PHRR and TSR of sample EP/5%EHP decreased by 20.5% and 20.7%, respectively. Moreover, MARHE, as an effective and comprehensive parameter to assess the heat release performance,[37] reduced from 445 kW m^{-2} of sample EP to 410 kW m^{-2} of sample EP/5%EHP, which further confirmed the positive effect of EHP on burning intensity of epoxy

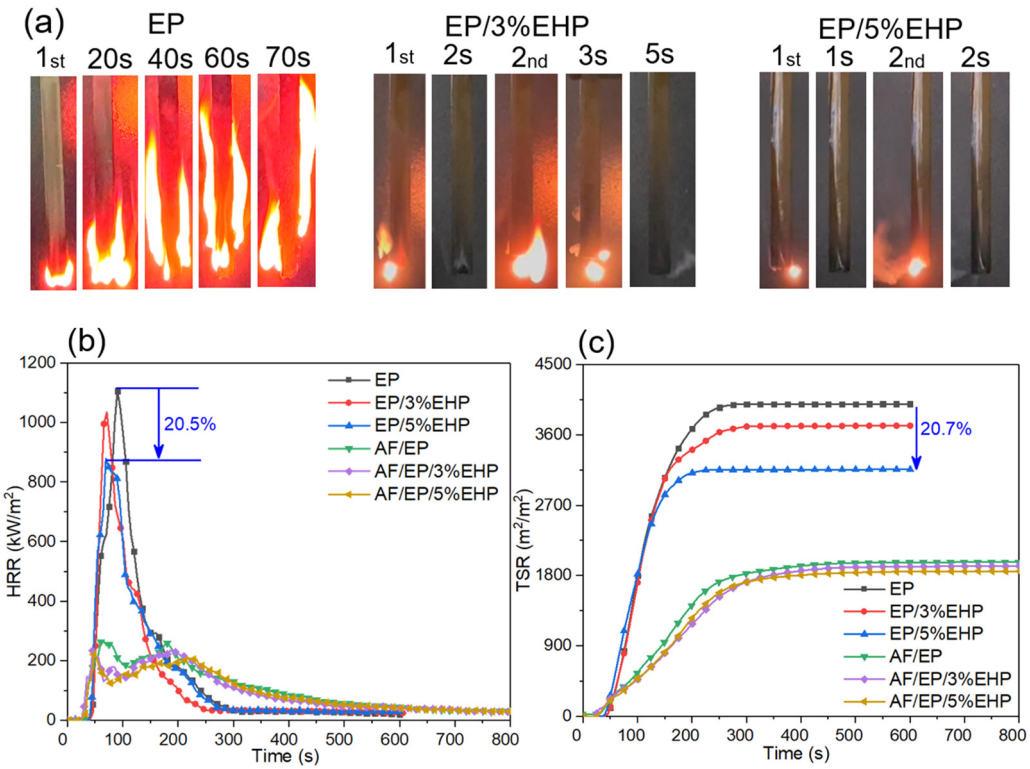

Fig. 4 (a) Digital images of EP samples during the UL-94 test, (b) HRR *vs.* time curves and (c) TSP *vs.* time curves from CCT.

Table 2 Data from CCT for EP and AF/EP samples

Sample	TTI (s)	PHRR (kW m^{-2})		MARHE (kW m^{-2})	THR (MJ m^{-2})	TSP (m^2)	av-EHC (MJ kg^{-1})	Residue (%)
EP	31 ± 1	1107 ± 15		445 ± 2	94 ± 3	35 ± 2	24.1 ± 0.6	2.0 ± 0.5
EP/3%EHP	32 ± 2	1035 ± 7		428 ± 4	89 ± 2	27 ± 2	23.8 ± 0.2	6.0 ± 0.6
EP/5%EHP	31 ± 2	879 ± 13		410 ± 3	80 ± 2	25 ± 1	22.9 ± 0.5	10.0 ± 0.1
AF/EP	27 ± 2	260 ± 8	264 ± 5	172 ± 5	76 ± 1	17 ± 1	24.4 ± 0.2	23.0 ± 0.5
AF/EP/3%EHP	25 ± 2	233 ± 6	229 ± 6	165 ± 2	73 ± 1	16 ± 1	24.3 ± 0.2	29.2 ± 0.6
AF/EP/5%EHP	26 ± 3	230 ± 7	226 ± 3	158 ± 4	73 ± 2	17 ± 2	24.5 ± 0.1	30.5 ± 0.5

resin. The TTI of epoxy resin was hardly affected by EHP. Additionally, the av-EHC decreased from 24.2 MJ kg^{-1} (EP) to 22.9 MJ kg^{-1} (EP/5%EHP) and residue increased from 2% (EP) to 10% (EP/5%EHP). The variation of av-EHC and residue indicates that the improved flame retardation is attributed to the positive actions from both gas and condensed phases. With regard to AF/EP laminates, there were two peaks of HRR at around 60 s and 180 s during combustion, which belonged to the heat release of epoxy resin and aramid fiber, respectively. Although there was some reduction in MARHE, the suppressed effect in heat release and smoke release behavior was not significant due to the ''wick-effect'' of aramid fiber.[38]

The flame-retardant mechanism was quantitatively evaluated according to eqn (1)–(3) and three main actions were discussed, involving flame inhibition, the charring effect, and the barrier effect.[39] Taking sample EP and sample EP/5%EHP as examples, the calculated values of flame inhibition, charring effect and barrier effect were 4.9%, 8.1%, and 6.7%, respectively. As for the laminate samples AF/EP and AF/EP/5%EHP, in which the PHRR value was the average of two peaks, the three corresponding values were −0.4%, 9.7%, and 9.4%. Based on the results above, the improved flame retardancy of epoxy resin mainly benefited from the charring and barrier effects, accompanied by certain flame inhibition action. However, almost no effect of flame inhibition was observed in the AF/EP system, and the other two action modes played a dominating role in the improvement of flame retardancy. Aiming to further understand the flame-retardant mechanism, PCFC was conducted to analyze the actions in gas and condensed phases. The PCFC method can assess the complete combustion of fuel gases generated from a material's decomposition, and the barrier effect can be negligible in PCFC. Therefore, the comparison of heat release behavior from CCT and PCFC was used to evaluate the gas-phase and barrier effect of EHP. The evaluation parameters were obtained from eqn (4),[40,41] and the R value calculated by the data from PCFC and CCT was named as $R1$ and $R2$, respectively. In Fig. 5(a), the PHRR value of sample EP/5%EHP from PCFC was 18.1% lower than that of sample EP, and the reduction was attributed to the quenching and dilution effect. Besides, $R1$ was higher than $R2$ due to the single action mode, and this comparison can highlight the existence of actions in gas and condensed phases during CCT. The earlier appearance of PHRR in sample EP/5%EHP was because of the charring process of epoxy resin catalyzed by EHP. As for AF/EP laminates in Fig. 5(b), the efficiency from gas-phase action can be negligible during combustion, and the difference of $R1$ and $R2$ further confirmed the presence of the protective effect from the compact charring layer. Furthermore, the gas-phase effect of EHP was confirmed *via* assessing results from TG-IR, listed in Fig. 5(c–f). Similar to the result from PCFC, the introduction of EHP led to the earlier decomposition and reduced the generation of total gas products, which was more obvious in epoxy resin than in the AF/EP system. However, the EHP did not change the decomposition route of EP and AF/EP, reflecting the same gas products. The char residue was also analyzed, as shown in Fig. 5(g–j). Compared with the surface of pure epoxy with massive holes, the modified sample exhibited more compact and continuous morphology with gas channels. With regard to the laminate, sample AF/EP showed a surface with obvious defects and loose yarns because the matrix burnt out during combustion. In contrast, sample AF/EP/5%EHP displayed a more continuous layer covered with massive chars.

$$\text{Flame inhibition} = 1 - \frac{\text{EHC(EP/EHP)}}{\text{EHC(EP)}} \quad (1)$$

$$\text{Charring effect} = 1 - \frac{\text{TML(EP/EHP)}}{\text{TML(EP)}} \quad (2)$$

$$\text{Barrier effect} = 1 - \frac{\text{PHRR(EP/EHP)}/\text{PHRR(EP)}}{\text{THR(EP/EHP)}/\text{THR(EP)}} \quad (3)$$

$$R = \frac{\text{PHRR(EP/EHP)}}{\text{PHRR(EP)}} \quad (4)$$

On the basis of the analysis above, the flame-retardant mechanism of EHP was highlighted by the combination of flame inhibition, charring and barrier effects. On the one hand, the decomposition of EHP produced a radical scavenger ($PO^{\bullet}$) to quench $HO^{\bullet}$ radicals from epoxy resin, along with a great amount of non-combustible gases (NH_3/H_2O) to dilute the concentration of fuels. Therefore, the flame inhibition effect was achieved in the gas phase. On the other hand, the decomposition of EHP promoted the dehydration and carbonization of epoxy resin to form a compact charring layer, which played a barrier role in the exchange process of heat and oxygen. Charring combined with the barrier effect resulted in the action mode in the condensed phase.

3.5. Mechanical properties of EP and AF/EP samples

First of all, the effect of EHP on the mechanical properties of epoxy resin was investigated through tensile and impact tests,

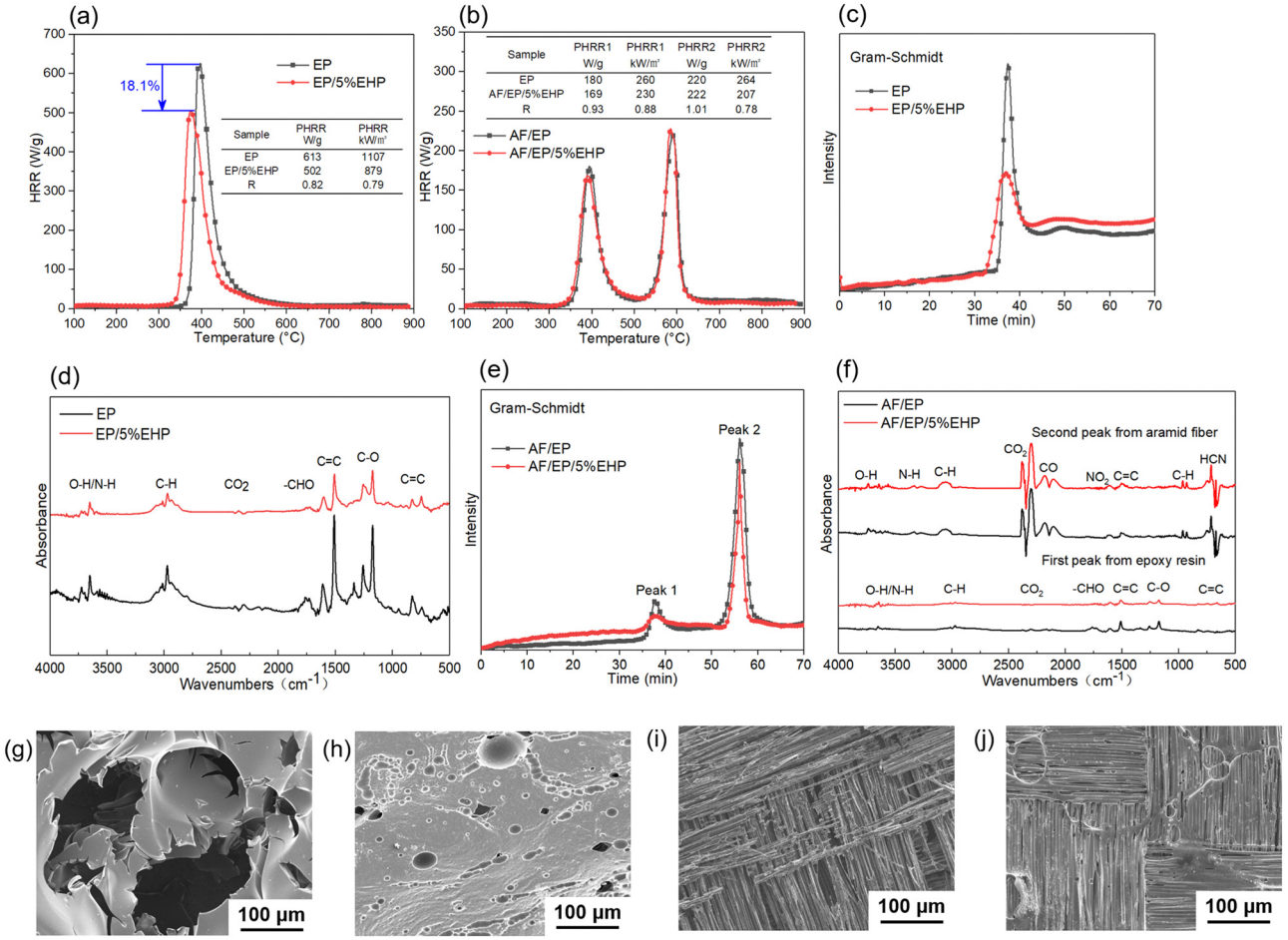

Fig. 5 Results from PCFC for EP samples (a) and AF/EP samples (b); TG-IR results: intensity *vs.* time curves of total gas products (c) and (e), FTIR spectra at maximum degradation rate (d) and (f); SEM images of char residue for sample EP (g), EP/5%EHP (h), AF/EP (i), and AF/EP/5%EHP (j).

Table 3 Mechanical data of EP and AF/EP

Sample	Tensile strength (MPa)	Young's modulus (GPa)	Elongation at break (%)	Impact strength (kJ m^{-2})	Interlaminar shear strength (MPa)
EP	71.2 ± 1.6	1.75 ± 0.05	8.6 ± 0.6	18.1 ± 3.0	N/A[a]
EP/3%EHP	82.2 ± 2.0	1.87 ± 0.05	8.1 ± 0.5	29.7 ± 2.0	N/A
EP/5%EHP	84.2 ± 2.5	1.98 ± 0.04	7.9 ± 0.3	29.1 ± 2.5	N/A
AF/EP	460 ± 10	24.8 ± 1.2	N/A	N/A	22.7 ± 0.9
AF/EP/3%EHP	478 ± 8	24.6 ± 1.3	N/A	N/A	24.1 ± 0.4
AF/EP/5%EHP	507 ± 7	24.7 ± 1.2	N/A	N/A	25.3 ± 0.4

[a] N/A: not applicable to this material.

as shown in Table 3. On increasing the loading of EHP, Young's modulus and elongation at break of epoxy thermosets exhibited upward and downward trends, respectively. This is attributed to the rigid structure of EHP that improves the stiffness and restricts the extension of the matrix at the same time. Besides, a positive effect was observed for tensile and impact strengths, which increased after incorporating EHP. Especially for sample EP/3%EHP, compared with sample EP, the tensile strength was 11 MPa higher and impact strength increased by 64%. Along with good dispersion, increased interfacial bonding, derived from π–π stacking of aromatic rings and hydrogen bonds from –NH– group, and the crack-toughening mechanism from microspheres brought out the outstanding strengthening and toughening effect for epoxy resin.

Due to the unbranched and inert molecular chains of aramid fiber, the incompatible interface between aramid fiber and epoxy resin usually becomes the key factor of poor mechanical properties.[42,43] Therefore, tensile and interlaminar shear strength (ILSS) tests were carried out to assess the effect of EHP on the mechanical behavior of the AF/EP composite, and the

corresponding data are listed in Table 3. Although the Young's modulus of the matrix increased after introducing EHP, there was almost no difference for that of the laminates with and without EHP. This is because the stiffness of AF/EP depends on the modulus of the fiber and matrix, while the modulus of EP is much lower than that of AF. Therefore, the modulus' variation of the matrix hardly affected the final results of AF/EP laminates. In contrast, the incorporation of EHP improved the tensile strength of AF/EP laminates, which increased from 460 MPa of sample AF/EP to 507 MPa of sample AF/EP/5%EHP. As the in-plane property, the tensile strength of the AF/EP laminate is affected by the reinforcement, matrix, and interfacial adhesion.[44] Based on the same conditions of the fiber, matrix and fabricating process, this enhancement phenomenon is attributed to the good interfacial bonding between AF and EP. From the profile photos of the AF/EP laminate after failure, presented in Fig. 6(a), it can be seen that delamination was improved in sample AF/EP/5%EHP. This insinuates that the interfacial adhesion was reinforced to effectively transfer load to dissipate more energy. Besides, the ILSS of AF/EP laminates was also increased after introducing EHP, and the value of sample AF/EP was 11.4% lower than that of sample AF/EP/5%EHP. In Fig. 6(b), similar ductile failure modes can be observed from the load-displacement curves due to inelastic deformation of aramid fibers. Relative to sample AF/EP, the treated samples can sustain a higher load and maintain a steady load after the maximum value. The response of the treated AF/EP laminate in a short beam shear test can be attributed to the enhanced adhesion and toughened matrix.[45]

In order to further reveal the strengthening and toughening mechanism, Fig. 6 illustrates the micromorphology of EP (c, d) and AF/EP (e, f) samples after failure. The untreated epoxy resin exhibited a typical brittle fracture mode, confirmed by a smooth surface with a straight propagation path of cracks. In contrast, the matrix with EHP showed a rougher morphology with lots of deflected cracks and crazing streaks, allowing a larger surface area to resist fracture. In the case of sample AF/EP, obvious delamination failure was observed, illustrated by the uncovered surface and clear gap of the fiber. After treating with EHP, the morphology became more complex,

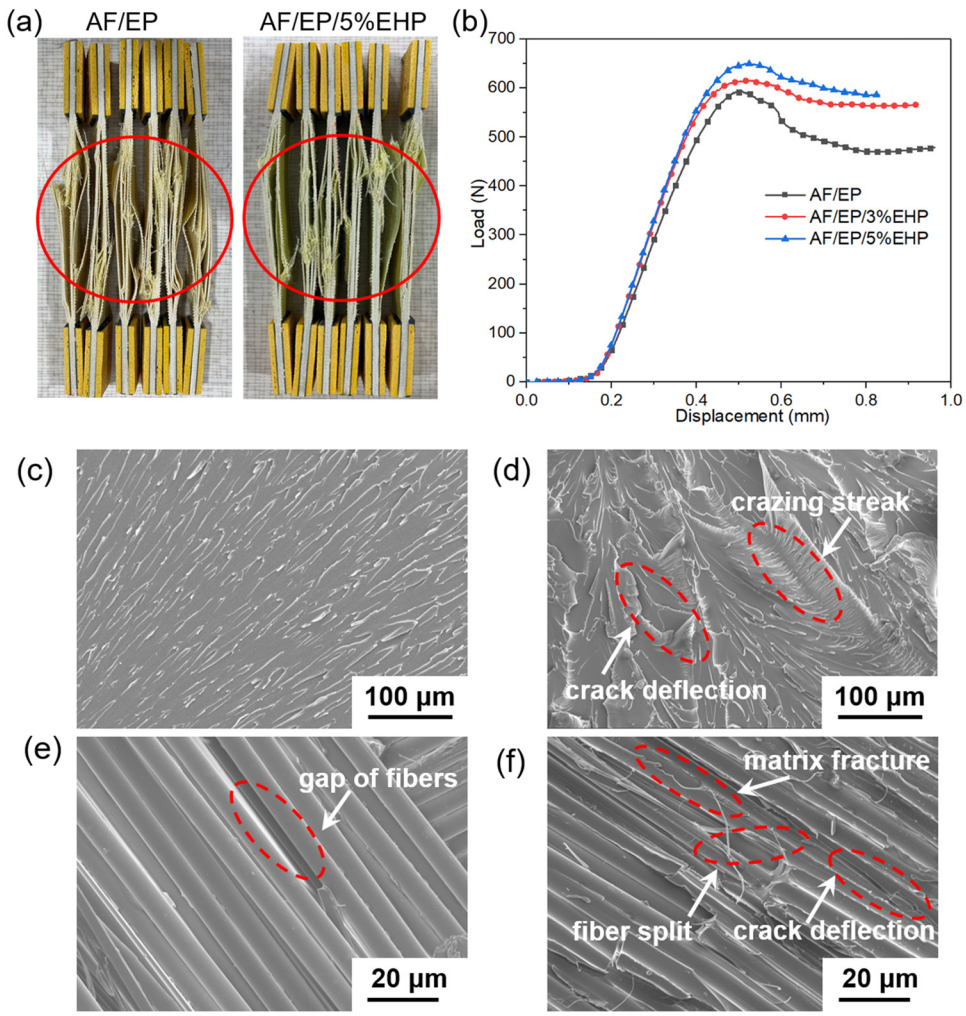

Fig. 6 Results of AF/EP samples from mechanical tests: (a) digital images after the tensile test, (b) load *vs.* displacement during the ILSS test; SEM images of EP (c) and EP/5%EHP (d) after the impact test; SEM images of AF/EP (e) and AF/EP/5%EHP (f) after the tensile test.

which was comprised of matrix fracture and crack deviation in addition to the original fiber split and delamination. This signals that the presence of EHP with functional groups can reinforce the interface strength between the fiber and matrix to convert the adhesion failure into a more cohesive one *via* chemical bonding. Therefore, the incorporation of EHP can reinforce and maintain the excellent mechanical properties of EP and AF/EP composites.

4. Conclusion

Cyclotriphosphazene and phosphaphenanthrene structures were combined to synthesize a multifunctional microsphere EHP, which was used to solve the issue between flame retardancy and mechanical properties of epoxy resin and its aramid fiber composite. Compared with pure epoxy resin with a LOI value of 25.5% and no rating in the UL-94 test, sample EP/5%EHP with only 0.65% P-loading had a higher LOI value of 34.5% and passed V-0 rating in the UL-94 test. The efficient flame retardancy was attributed to the combination of multiple action modes, contributed by flame inhibition (4.9%), and charring (8.1%) and barrier (6.7%) effects. The introduction of EHP endowed epoxy resin with good compatibility and excellent interfacial bonding. Consequently, the tensile and impact strengths of sample EP/5%EHP increased by 13 MPa and 60.7%, respectively. Moreover, the modified epoxy thermosets maintained good thermal stability. With regard to AF/EP composites, the improvement was obtained in both burning behavior and mechanical properties. Compared with sample AF/EP, the introduction of 5 wt% EHP weakened the burning intensity (MARHE decreased by 8%), as well as increased the tensile strength and interlaminar shear strength by 47 MPa and 2.6 MPa, respectively. These results suggested that tailoring the chemical structure of the compound can optimize the flame-retardant action mode and interface performance, which finally achieved efficient flame retardancy and mechanical enhancement for epoxy resin and its aramid fiber composite.

Conflicts of interest

The authors declare that they have no known competing financial interests or personal relationships that could have appeared to influence the work reported in this paper.

Acknowledgements

The authors are grateful to the Science and Technology Innovation Program of Chongqing and the National Natural Science Foundation of China (NSFC) for this work through Grant No. 2022ZX1200018 and 12102054, respectively. This study was also supported by other members from the State Key Laboratory of Explosion Science and Safety Protection.

References

1 K. Song, Y. T. Pan, J. Zhang, P. Song, J. He, D. Y. Wang and R. Yang, Metal–Organic Frameworks–Based Flame-Retardant System for Epoxy Resin: A Review and Prospect, *Chem. Eng. J.*, 2023, **468**, 143653.
2 R. Wazalwar, M. Sahu and A. M. Raichur, Mechanical properties of aerospace epoxy composites reinforced with 2D nano-fillers: current status and road to industrialization, *Nanoscale Adv.*, 2021, **3**, 2741–2776.
3 C. Yu, P. Yu, G. Ma, L. Zhou, F. Deng, F. Wang and X. Zhu, Preparation of aramid-based epoxy resin from low-grade aramid, *RSC Adv.*, 2021, **11**, 36265–36272.
4 V. Unnikrishnan, O. Zabihi, M. Ahmadi, Q. Li, P. Blanchard, A. Kiziltas and M. Naebe, Metal-organic framework structure-property relationships for high-performance multifunctional polymer nanocomposite applications, *J. Mater. Chem. A*, 2021, **9**, 4348–4378.
5 J. Wang, X. Chen, J. Wang, S. Yang, K. Chen, L. Zhu, S. Huo, P. Song and H. Wang, High-performance, intrinsically fire-safe, single-component epoxy resins and carbon fiber reinforced epoxy composites based on two phosphorus-derived imidazoliums, *Polym. Degrad. Stab.*, 2023, **208**, 110261.
6 Y. Xiao, X. Mu, B. Wang, W. Hu, J. Wang, F. Zhou, C. Ma, Y. Hu and L. Song, A novel phosphorous-containing polymeric compatibilizer: Effective reinforcement and flame retardancy in glass fiber reinforced polyamide 6 composites, *Composites, Part B*, 2021, **205**, 108536.
7 Y. Han, Y. Xu, Y. Liu, Q. Wang, Z. Zhang and Z. Wang, An efficient interfacial flame-resistance mode to prepare glass fiber reinforced and flame retarded polyamide 6 with high performance, *J. Mater. Chem. A*, 2013, **1**, 10228–10233.
8 Y. Luo, J. Cai, L. Li, X. Lin, L. Xiao and L. Hou, Multi-DOPO-based derivative for enhancing flame retardancy and mechanical properties of epoxy resin, *Prog. Org. Coatings*, 2023, **184**, 107862.
9 Z. Chi, Z. Guo, Z. Xu, M. Zhang, M. Li, L. Shang and Y. Ao, A DOPO-based phosphorus-nitrogen flame retardant bio-based epoxy resin from diphenolic acid: Synthesis, flame-retardant behavior and mechanism, *Polym. Degrad. Stab.*, 2020, **176**, 109151.
10 Y. Guo, H. Rong, Z. Chen, T. Chen, Y. Yu, X. Zhang, Y. Chu, Q. Zhang, C. Li and J. Jiang, A novel DOPO derivative containing multifunctional groups aiming to improve fire safety, thermal stability and curing state towards epoxy resin, *Polym. Degrad. Stab.*, 2022, **205**, 110142.
11 Y. Yang, D. Y. Wang, R. K. Jian, Z. Liu and G. Huang, Chemical structure construction of DOPO-containing compounds for flame retardancy of epoxy resin: A review, *Prog. Org. Coatings*, 2023, **175**, 107316.
12 Y. Yang, Z. Li, G. Wu, W. Chen and G. Huang, A novel biobased intumescent flame retardant through combining simultaneously char-promoter and radical-scavenger for the application in epoxy resin, *Polym. Degrad. Stab.*, 2022, **196**, 109841.
13 C. Bao, Y. Guo, B. Yuan, Y. Hu and L. Song, Functionalized graphene oxide for fire safety applications of polymers:

A combination of condensed phase flame retardant strategies, *J. Mater. Chem.*, 2012, **22**, 23057–23063.

14 Y. Wang, S. Han, X. Hu, W. Li, B. Na, C. Xie and X. Wang, Benefiting from the multiple effects of ferrocene and cyclotriphosphazene bi-based hierarchical layered nanosheets towards improving fire safety and mechanical properties of epoxy resin, *Composites, Part B*, 2023, **264**, 110914.

15 P. Liu, L. Wang, Y. Yang, Y. Qu and L. J. Ming, Recent advances of cyclotriphosphazene derivatives as fluorescent dyes, *Dyes Pigm.*, 2021, **188**, 109214.

16 T. N. Thompson, S. Ramos-Hunter, J. Robertson and N. Y. Arnett, Interfacial synthesis of bisphenol A tetrachlorocyclotriphosphazene from bisphenol A and hexachlorocyclotriphosphazene, *Tetrahedron Lett.*, 2013, **54**, 5311–5313.

17 Y. Wei, S. Zhu, Q. Qian, Q. Jiang, L. Zhang, K. Jin, W. Liu and Y. Qiu, Hexachlorocyclotriphosphazene functionalized lignin as a sustainable and effective flame retardant for epoxy resins, *Ind. Crops Prod.*, 2022, **187**, 115543.

18 J. Liu, Z. He, G. Wu, X. Zhang, C. Zhao and C. Lei, Synthesis of a novel nonflammable eugenol-based phosphazene epoxy resin with unique burned intumescent char, *Chem. Eng. J.*, 2020, **390**, 124620.

19 J. Hong, T. Wu, H. Wu, B. Zeng, S. Zeng, T. Chen, X. Wang, Z. Lu, C. Yuan, K. Balaji, D. F. S. Petri and L. Dai, Nanohybrid silver nanoparticles@halloysite nanotubes coated with polyphosphazene for effectively enhancing the fire safety of epoxy resin, *Chem. Eng. J.*, 2021, **407**, 127087.

20 M. Zhou, D. Zeng, S. Qiu, X. Zhou, L. Cheng, Z. Xu, W. Xing and Y. Hu, Amino-functionalized carbon nanotubes/polyphosphazene hybrids for improving the fire safety and mechanical properties of epoxy, *Prog. Nat. Sci. Mater. Int.*, 2022, **32**, 179–189.

21 C. Wang, S. Huo, G. Ye, B. Wang, Z. Guo, Q. Zhang, P. Song, H. Wang and Z. Liu, Construction of an epoxidized, phosphorus-based poly(styrene butadiene styrene) and its application in high-performance epoxy resin, *Composites, Part B*, 2024, **268**, 111075.

22 Y. Zhao, X. Li, J. Shen, C. Gao and B. Van Der Bruggen, The potential of Kevlar aramid nanofiber composite membranes, *J. Mater. Chem. A*, 2020, **8**, 7548–7568.

23 C. Yang, J. Dong, Y. Fang, L. Ma, X. Zhao and Q. Zhang, Preparation of novel low-: κ polyimide fibers with simultaneously excellent mechanical properties, UV-resistance and surface activity using chemically bonded hyperbranched polysiloxane, *J. Mater. Chem. C*, 2018, **6**, 1229–1238.

24 T. Linhares, M. T. Pessoa De Amorim and L. Durães, Silica aerogel composites with embedded fibres: A review on their preparation, properties and applications, *J. Mater. Chem. A*, 2019, **7**, 22768–22802.

25 Q. Wu, B. Xiao, Q. Liu, H. Deng, Z. Ye, Y. Li, R. Yao and J. Zhu, New strategy for enhancing interfacial adhesion between carbon fiber and epoxy by using mussel-inspired polydopamine-Fe complex nanospheres, *Composites, Part B*, 2023, **266**, 111032.

26 Y. Yang, W. Chen, Z. Li, G. Huang and G. Wu, Efficient flame retardancy, good thermal stability, mechanical enhancement, and transparency of DOPO-conjugated structure compound on epoxy resin, *Chem. Eng. J.*, 2022, **450**, 138424.

27 M. Basharat, Y. Abbas, W. Liu, Z. Ali, S. Zhang, W. Zou, Z. Wu and D. Wu, Unusual excitation wavelength tunable multiple fluorescence from organocyclo-phosphazene microspheres: Crosslinked structure-property relationship, *Polymer*, 2019, **185**, 121942.

28 L. Chen, Q. Jiang, Z. Luo and B. Wang, Facile synthesis of a reactive P/N/S-containing compound toward highly effective flame retardancy of epoxy resin with high transparency and improved mechanical strength, *Fire Saf. J.*, 2021, **126**, 103472.

29 Y. F. Ai, L. Xia, F. Q. Pang, Y. L. Xu, H. B. Zhao and R. K. Jian, Mechanically strong and flame-retardant epoxy resins with anti-corrosion performance, *Composites, Part B*, 2020, **193**, 108019.

30 R. Liu and X. Wang, Synthesis, characterization, thermal properties and flame retardancy of a novel nonflammable phosphazene-based epoxy resin, *Polym. Degrad. Stab.*, 2009, **94**, 617–624.

31 T. N. Thompson, S. Ramos-Hunter, J. Robertson and N. Y. Arnett, Interfacial synthesis of bisphenol A tetrachlorocyclotriphosphazene from bisphenol A and hexachlorocyclotriphosphazene, *Tetrahedron Lett.*, 2013, **54**, 5311–5313.

32 B. Wang, Y. Zhang, J. Li, Z. Fang, Z. Guo and S. Ran, Preparation and Characterization of Transparent Polycarbonate with High Flame Retardancy and Smoke Suppression, *ACS Appl. Polym. Mater.*, 2023, **5**, 6463–6471.

33 C. Liu, H. Yan, Q. Lv, S. Li and S. Niu, Enhanced tribological properties of aligned reduced graphene oxide-Fe3O4@polyphosphazene/bismaleimides composites, *Carbon*, 2016, **102**, 145–153.

34 Y. Sui, H. Sima, W. Shao and C. Zhang, Novel bioderived cross-linked polyphosphazene microspheres decorated with FeCo-layered double hydroxide as an all-in-one intumescent flame retardant for epoxy resin, *Composites, Part B*, 2022, **229**, 109463.

35 S. Huo, T. Sai, S. Ran, Z. Guo, Z. Fang, P. Song and H. Wang, A hyperbranched P/N/B-containing oligomer as multifunctional flame retardant for epoxy resins, *Composites, Part B*, 2022, **234**, 109701.

36 D. Griffin, S. Wood and I. Hamerton, Measurement of the glass transition temperature of an epoxy resin using principal components of Raman spectra, *Composites, Part B*, 2020, **200**, 108210.

37 D. Jia Chen, Y. Lu Zhang, J. Yu He and X. Mei Li, Making polycarbonate flame retardant: Flame retardant selection and calorimetric analyses, *Polym. Test.*, 2023, **117**, 107876.

38 Q. R. Ren, S. Gu, J. H. Liu, Y. Z. Wang and L. Chen, Catalyst-free reprocessable, degradable and intrinsically flame-retardant epoxy vitrimer for carbon fiber reinforced composites, *Polym. Degrad. Stab.*, 2023, **211**, 110315.

39 S. Tang, V. Wachtendorf, P. Klack, L. Qian, Y. Dong and B. Schartel, Enhanced flame-retardant effect of a montmorillonite/phosphaphenanthrene compound in an epoxy thermoset, *RSC Adv.*, 2017, **7**, 720–728.

40 R. Sonnier, L. Ferry, C. Longuet, F. Laoutid, B. Friederich, A. Laachachi and J. M. Lopez-Cuesta, Combining cone calorimeter and PCFC to determine the mode of action of flame-retardant additives, *Polym. Adv. Technol.*, 2011, **22**, 1091–1099.
41 M. Kervran, M. Shabanian, C. Vagner, M. Ponçot, J. Meier-Haack, F. Laoutid, S. Gaan and H. Vahabi, Flame retardancy of sustainable polylactic acid and polyhydroxybutyrate (PLA/PHB) blends, *Int. J. Biol. Macromol.*, 2023, **251**, 126208.
42 X. Zhu, L. Yuan, G. Liang and A. Gu, Unique surface modified aramid fibers with improved flame retardancy, tensile properties, surface activity and UV-resistance through in situ formation of hyperbranched polysiloxane-Ce0.8Ca0.2O1.8 hybrids, *J. Mater. Chem. A*, 2015, **3**, 12515–12529.
43 X. Zhu, L. Yuan, G. Liang and A. Gu, Unique UV-resistant and surface active aramid fibers with simultaneously enhanced mechanical and thermal properties by chemically coating Ce 0.8Ca0.2O1.8 having low photocatalytic activity, *J. Mater. Chem. A*, 2014, **2**, 11286–11298.
44 R. Guzman de Villoria, P. Hallander, L. Ydrefors, P. Nordin and B. L. Wardle, In-plane strength enhancement of laminated composites via aligned carbon nanotube interlaminar reinforcement, *Compos. Sci. Technol.*, 2016, **133**, 33–39.
45 J. Nasser, K. Steinke, L. Zhang and H. Sodano, Enhanced interfacial strength of hierarchical fiberglass composites through an aramid nanofiber interphase, *Compos. Sci. Technol.*, 2020, **192**, 108109.